Scientific Research Publishing

Smart Grid and Renewable Energy, 2018, 9, 101-112
http://www.scirp.org/journal/sgre
ISSN Online: 2151-4844
ISSN Print: 2151-481X

Droop Control Methods for PV-Based Mini Grids with Different Line Resistances and Impedances

Nicholas Nixon Opiyo

Centre for Integrated Energy Research, School of Chemical and Process Engineering, University of Leeds, Leeds, England
Email: Nicholas.Opiyo1@gmail.com

How to cite this paper: Opiyo, N.N. (2018) Droop Control Methods for PV-Based Mini Grids with Different Line Resistances and Impedances. *Smart Grid and Renewable Energy*, **9**, 101-112.
https://doi.org/10.4236/sgre.2018.96007

Received: May 7, 2018
Accepted: June 12, 2018
Published: June 15, 2018

Abstract

Different droop control methods for PV-based communal grid networks (minigrids and microgrids) with different line resistances (R) and impedances (X) are modelled and simulated in MATLAB to determine the most efficient control method for a given network. Results show that active power-frequency (P-f) droop control method is the most efficient for low voltage transmission networks with low X/R ratios while reactive power-voltage (Q-V) droop control method is the most efficient for systems with high X/R ratios. For systems with complex line resistances and impedances, *i.e.* near unity X/R ratios, P-f or Q-V droop methods cannot individually efficiently regulate line voltage and frequency. For such systems, P-Q-f droop control method, where both active and reactive power could be used to control PCC voltage via shunt-connected inverters, is determined to be the most efficient control method. Results also show that shunt-connection of inverters leads to improved power flow control of interconnected communal grids by allowing feeder voltage regulation, load reactive power support, reactive power management between feeders, and improved overall system performance against dynamic disturbances.

Keywords

Droop Control, Communal Grid, Inverter

1. Introduction

A PV-based communal grid can be defined as a collection of distributed PV systems, distributed energy storage devices, and distributed loads, operating as a single and controllable system capable of supplying power to an area of service. They should be operable in both grid-connected and islanded modes. Power

electronics interfaces and controllers are used in communal grids to ensure quality, reliable and independent power supply at all times. A control system must be able to disconnect and reconnect the communal grid from the utility grid, maintain voltage and frequency levels in islanded mode of operation, and facilitate a black start after a system failure [1]. The main drivers of communal grids are demand, cost, technical aspects, and environmental concerns [2]. These factors influence the control strategy applied for a communal grid and will need to give consideration to issues such as load sensitivity, number of distributed generators in the communal grid, power quality requirements, ownership of the communal grid and distributed generators, distances between the distributed generators, the existing communication infrastructure, each distributed generator's energy source, and whether the communal grid is predominantly and exporter or importer of electricity [3] [4] [5].

1.1. Droop Control

Droop control method is the most widely used in PV power systems to enable automatic load sharing between different distributed PV systems and to extend operating range of active (P) and reactive (Q) power ratings of a given inverter [6] [7]. The method requires P and Q to be measured in order to droop the frequency (f) and voltage (V) accordingly such that the inverter mimics the behaviour of a synchronous generator [6] [7]. A reactive power voltage (Q-V) droop control is used to control point of common coupling (PCC) voltage magnitude while an active power frequency (P-f) droop control is used to control the frequency of the system in islanded mode [6]. For easy analysis, we consider a two-bus synchronous generator connected to a high voltage (HV) transmission network as shown in **Figure 1**.

The power produced at the generator terminal is expressed as [8]:

$$P = \frac{E}{R^2 + X^2}\left[XV\sin\delta + R\left(E - V\cos\delta\right)\right] \tag{1}$$

$$Q = \frac{E}{R^2 + X^2}\left[-RV\sin\delta + X\left(E - V\cos\delta\right)\right] \tag{2}$$

where δ is the voltage angle.

Since HV networks have high reactance (X) and low line resistance (R), and thus high X/R ratios, the line resistance can be ignored and Equations (1) and (2) reduced to [8]:

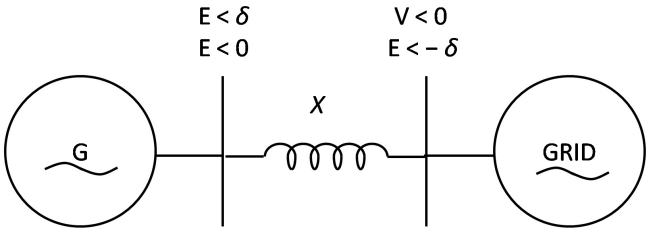

Figure 1. Generator connected to grid.

$$P = \frac{VE\sin\delta}{X} \tag{3}$$

$$Q = \frac{E^2 - VE\cos\delta}{X} \tag{4}$$

Usually, δ is very small (zero) and therefore $\cos\delta \cong 1$ and $\sin\delta \cong \delta$. Equations (3) and (4) can therefore be simplified further to [8]:

$$\delta \approx \frac{PX}{VE} \tag{5}$$

$$E - V \approx \frac{QX}{E} \tag{6}$$

The reactive power Q can therefore be controlled by the difference in voltage between E and V, and the active power P, by the voltage angle δ. The voltage angle δ can be expressed in terms of angular frequency ω (radians/second), and therefore in terms of electrical frequency f (hertz) as [9]:

$$\delta = \int \Delta\omega \mathrm{d}t = \frac{1}{2\pi}\int \Delta f \mathrm{d}t \tag{7}$$

The relationship outlined above allows automatic load sharing between many synchronous generators (SGs) when combined with P-f droop control as shown in **Figure 2(a)** [1] [2]; a change in load will cause frequency variation at the terminal of each SG. Active power will flow from regions of higher frequency to regions of lower frequency. Frequency variations within the network will eventually drift to an average steady state value [2]. The new steady state frequency will be proportional to the change in power, as shown in **Figure 2(b)** [1].

1.2. Inverter Controls

Inverters are used to interface communal grids with utility grids and can be classified according to modes of operation as PQ or V-f (also known as voltage source inverter (VSIs)). A PQ inverter controls the real (P) and reactive (Q) power by adjusting the magnitude of the output real and reactive current. It therefore operates as a voltage controlled current source [10]. A voltage source inverter controls the voltage (V) and frequency (f) at the output terminal, and thus operates as a voltage source [9] [10]. The mode of an inverter operation is

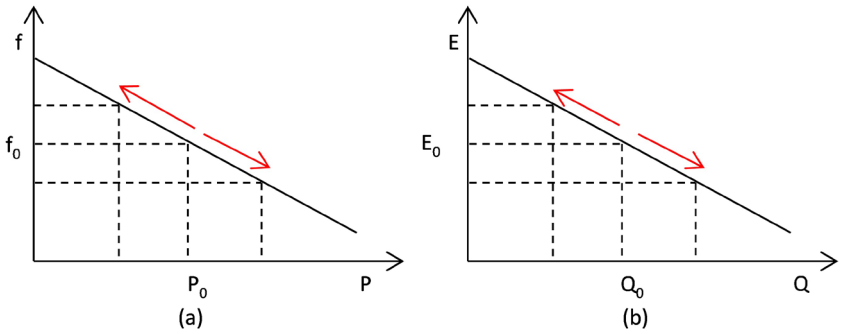

Figure 2. P-f and Q-V droops.

chosen depending on a communal grid's architecture and control strategy, and may change depending on whether the communal grid is islanded or grid-connected. Unlike synchronous generators, inverters do not have rotors and thus no natural connection between frequency and active power. To achieve stable operation with multiple distributed PV systems, the inverters are controlled so that they mimic the characteristics of synchronous generators with P-f and Q-V droop controls [11]. For a PQ inverter, these droops are implemented as (f) and (V) functions, whereas a VSI uses (P) and (Q) droops [12].

1.2.1. PQ Inverter with Droop Control

As opposed to a synchronous generator that uses its rotor speed as the frequency input for the P-f droop controller, a PQ inverter does not set the frequency, but rather measures the grid frequency using a phase lock loop (PLL) and then operates at that measured frequency [9] [10] [11]. The inverter will adjust its power accordingly, by comparing the measured frequency to a reference (nominal grid frequency) value accordingly. This relationship is modelled as [9] [10] [11]:

$$P(f) = P_0 - (f_{set} - f)k_f \tag{8}$$

where P_0 is the power delivered by the inverter at setpoint frequency f_{set} and k_f is the gradient of the droop, which determines how much the active power P will change in response to a change in frequency f. When a Q-V droop is used, the PQ inverter measures the terminal voltage and compares this to the reference value. The reactive power is adjusted by altering the reactive component of the inverter current [10]. This reactive power adjustment is expressed as [9] [10] [11]:

$$Q(V) = Q_0 - (V_{set} - V)k_v \tag{9}$$

where Q_0 is the reactive power delivered/consumed by the inverter at setpoint voltage V_{set} and k_v is the gradient of the droop, which determines how much the reactive power Q will change in response to a change in voltage V.

1.2.2. VSI Inverter with Droop Control

A VSI with droop control uses measured active power output to generate the VSI frequency and measured reactive power output to generate the VSI voltage [8]. It thus operates like a synchronous generator. This process can be modelled by Equations (10) and (11) below [8]:

$$f(P) = (P_0 - P)k_p - f_{set} \tag{10}$$

where k_p is the gradient of the droop, which determines how much the frequency will change in response to a change in power P.

$$V(Q) = (Q_0 - Q)k_q - V_{set} \tag{11}$$

where k_q is the gradient of the droop, which determines how much the voltage will change in response to a change in reactive power Q.

The conventional droop control relies on the inductive nature of transmission lines and is thus based on the assumption that the line resistance (R) is much less

than the reactance (X), *i.e.*, high X/R ratio and therefore active power flow is predominately a function of the voltage angle (δ) [12]. This is the case for high voltage (HV) and medium voltage (MV) lines, but it is not so for low voltage (LV) networks as shown in Table 1.

For systems with LV transmission networks and thus high line resistance, the low X/R ratio causes a coupling effect between active and reactive power, rendering Q-V droop control method ineffective in achieving required voltage regulation in such systems [14]. A solution to this problem has been proposed by Alatrash *et al.*, in which a control system that incorporates virtual reactance at the terminals of the VSI is used [15]. The idea behind this method is to emulate the higher reactance of MV and HV distribution lines. Abusara *et al.* proposed a control strategy that employs both virtual inductance to remove harmonic disturbances and a real-time integration filter to eliminate the need for measuring average power [16].

2. Methodology

Consider a communal grid with two-feeder distribution systems as shown in Figure 3 below. The two inverters in the systems are connected in parallel through switch S_4; parallel connection of the inverters enables them to control both active and reactive power flow through shunt-connected transformers, leading to overall improved system performance [17]. The necessary active power for the compensation is drawn from the interconnected feeders via the inverters. The controller then circulates minimum active power between the feeders while the active and reactive power droop coefficients are adjusted online

Table 1. Typical Line Parameters [13].

Type of line	R (Ω/km)	X (Ω/km)	R/X
Low voltage	0.642	0.083	7.7
Medium voltage	0.161	0.190	0.85
High voltage	0.06	0.191	0.31

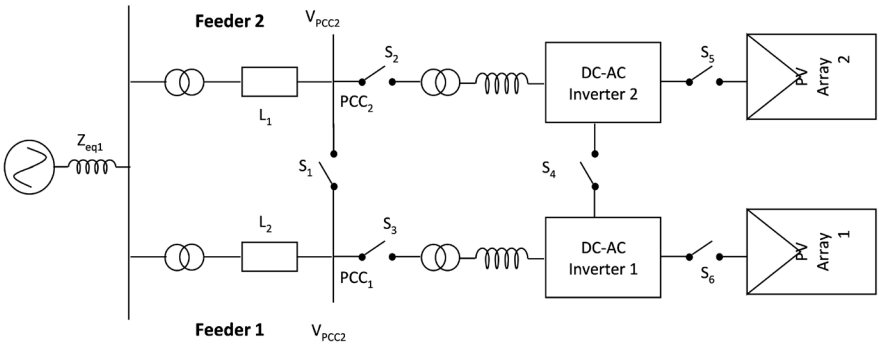

Figure 3. Interline-PV (I-PV) System Configuration.

through a look up table based on the PCC voltage level. A real-time integration inductor-capacitor-inductor (LCL)-filter with a virtual inductance is used to actively damp the inverter output without the need for extra sensors to feedback measured signals. Impact of DC link voltage and resonance frequency on stability would then be analysed.

The PV system does not produce real power during the night and therefore switches S_5 and S_6 can be opened. During the day when the PV system generates power, switches S_2 - S_6 are closed, while switch S_1 is kept open in order to operate the system as interline-PV (I-PV), controlled through an interline power flow controller (IPFC) [18]. Let's set the voltage levels of both the feeders at 25 kV and the acceptable range of PCC voltage variation at ±5%. Let's consider the loads at the ends of feeder 1 and 2 as P and Q, respectively, and let's assume that they have different values. If inverters 1 and 2 are each rated at 2 MVA then only a maximum of 1 MW active power can circulate between feeders 1 and 2 through the inverters. This is to avoid considerable voltage drop on the other feeder from which the active power is to be taken. The PCC voltages at feeders 1 and 2 are expressed as V_{pcc1} and V_{pcc2}, respectively. The active and reactive powers injected or absorbed by feeders 1 and 2 are expressed as P_{inv1}, Q_{inv1}, P_{inv2} and Q_{inv2} respectively. The reactive powers supported by the inverters are shown as positive quantities since they are leading, while the reactive powers are shown as negative quantities since they are lagging. For simplicity, the simulation results are expressed in per unit (*pu*), with base voltage of 25 kV and base power of 1 MVA. Feeders 1 and 2 line parameters are: 0.08 + j0.04 ohm/km and line lengths: $L_1 = L_2 = 20$ km.

Figure 4 shows a Thevenin equivalent of feeder 2 connected to inverter 2. The figure represents a power source ($E_{PV}\angle\phi$) where Z_{th} represents the feeder as well as inverter coupling impedance, ϕ is the phase angle difference between PCC and grid voltages, while θ is the impedance angle due to Z_{th}.

The following equations are used to control the active and reactive power flows ($S = P + jQ$) from inverter 2 (the power source) to feeder 2 (the grid):

$$P = \frac{V_{th}}{Z_{th}}\left[\left(E_{PV}\cos\phi - V_{th}\right)\cos\theta + E_{PV}\sin\theta\sin\phi\right] \tag{12}$$

$$Q = \frac{V_{th}}{Z_{th}}\left[\left(E_{PV}\cos\phi - V_{th}\right)\sin\theta - E_{PV}\cos\theta\sin\phi\right] \tag{13}$$

Since ϕ is usually very small, *i.e.*, $\cos\phi \approx 1$, and $\sin\phi \approx \phi$, the equations above are reduced to:

$$P = \frac{V_{th}}{Z_{th}}\left[\left(E_{PV} - V_{th}\right)\cos\theta + E_{PV}\phi\sin\theta\right] \tag{14}$$

$$Q = \frac{V_{th}}{Z_{th}}\left[\left(E_{PV} - V_{th}\right)\sin\theta - E_{PV}\phi\cos\theta\right] \tag{15}$$

Equations (14) and (15) show the dependency of delivered active and reactive power on the impedance angle θ and the phase difference angle ϕ.

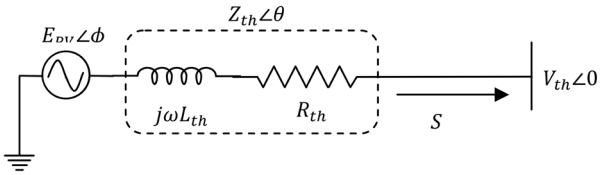

Figure 4. Thevenin Equivalent Circuit of Feeder 2 Connected to Inverter 2.

2.1. P-f Droop Control Method

This method is suitable for networks with high resistive values and low reactance, *i.e.* low *X*/*R* ratios. This makes the impedance angle θ equals to zero hence, from Equation (14), the active power delivered by the inverter is proportional to the voltage difference ($E_{PV} - V_{th}$) and thus proportional to the inverter E_{PV}. The reactive power of inverter 2 is proportional to the phase difference angle ϕ, *i.e.* proportional to the frequency *f* of the system. It should be noted that ϕ is varying within a small range. *P* remains constant irrespective of any change in ϕ while *Q* significantly changes with changing ϕ. On the other hand, *P* significantly increases with increasing E_{PV} while *Q* is hardly affected by changes in E_{PV}.

2.2. Q-V Droop Control Method

This method is suitable for networks with high *X*/*R* ratios, *i.e.* low line resistance and high reactance and thus the impedance angle θ goes to 90˚. The reactive power of the inverter is proportional to the inverter voltage E_{PV} and the active power is proportional to the frequency *f*. *P* significantly changes with changing ϕ while *Q* remains constant regardless of any changes in ϕ. On the other hand, *P* hardly changes with changing E_{PV} while *Q* significantly changes with E_{PV}. The *Q*-*V* droop control method is one of the widely used methods for voltage regulation; unlike the *P*-*f* droop method where additional provision for real power is required; *Q*-*V* droop method does not need such a source of real power for generating the necessary *Q* for compensation.

2.3. P-Q-V Droop Control Method

This method is suitable for systems with complex line impedances, *i.e.* where neither the line resistance nor the reactance is more significant over the other and therefore neither can be ignored. In such systems, the *X*/*R* ratio is near unity and therefore neither the *P*-*f* nor the *Q*-*V* droop method is sufficient to regulate the PCC voltage. In this system both the active and reactive power are simultaneously affected by changes in voltage magnitude E_{PV} and the phase difference angle ϕ. Since in these systems both active and reactive power affect the voltage magnitude, the system can be represented by the following equation [18]

$$V = V_{pcc} - (n_L * P) - j(m_L * Q) \tag{16}$$

where n_L and m_L are the electric load droop coefficients while V_{pcc} is the voltage before compensation and is given by

$$V_{pcc} = V_{ref} + (n_d * P) + j(m_d * Q) \tag{17}$$

where n_d and m_d are the active and reactive power coefficients for the proposed *P-Q-V* droop method while V_{ref} is the desired reference value of PCC voltage, *i.e.* 1 *pu* (25 kV).

3. Results and Discussion

For simplicity only feeder 2 in Figure 3 is regulated. If PCC voltage rises by more than 5%, another distributed PV generator is used to inject active power into the system while if PCC voltage drops below 5% a heavy load is connected to feeder 2. At t_1 (0.0 S), inverter 2 starts operation to regulate feeder 2 PCC voltage based on *P-f*, *Q-V*, or *P-Q-V* droop control methods with normal loads. At t_2 (0.5 S) feeder 2 PCC is increased above 5% due to active power injected from another PV source. At t_3 (1.0 S) feeder 2 PCC voltage is decreased below 5% limit due to increased load and no additional active power injection.

3.1. System Performance with P-f Droop Control Method

Figure 5 shows the performance of feeder 2 at t_1, t_2, and t_3. The PCC voltage is regulated according to the P-f droop control method. Figure 5(a) shows the PCC voltage before and after compensation, Figure 5(b) shows the PCC voltage before and after active and reactive powers injected by inverter 2, Figure 5(c) shows the circulated active power between feeder 1 and feeder 2, and Figure 5(d) shows the apparent power S circulated through inverter 2 with respect to its rated capacity of 2 MVA. From t_1 to t_2, the PCC voltage is 1.035 *pu*, and it is reduced to 1.015 *pu* using *P-f* droop method; 0.6 *pu* of active power is absorbed through inverter 2 and is drawn from feeder 1. From t_2 to t_3, the PCC voltage is increased to 1.089 *pu* and it is reduced to 1.06 *pu*. This is done by absorbing 1 *pu* active power. Even though inverter 2 could absorb up to 2 *pu* to regulate the PCC voltage, it has been limited to a maximum of 1 *pu* for active power injection in order not to overload feeder 1 and thus to maintain its voltage within acceptable limits. From t_3 to 1.4 sec, the PCC voltage falls to 0.925 *pu* due to heavy load on feeder 2. Inverter 2 then injects maximum allowable 1 *pu* active power to improve the PCC voltage from 0.925 to 0.945 *pu*. The droop coefficient for this method is 0.02 *pu*/*MW* for all the operating conditions.

3.2. System Performance with Q-V Droop Control Method

Figure 6 shows the performance of feeder 2 with *Q-V* droop control method. The conditions for the PCC voltage before compensation are kept identical to that for *P-f* droop method. From t_1 to t_2 the PCC voltage is reduced from 1.035 *pu* to 1.02 *pu* as shown in Figure 6(a) by injecting 1.0 *pu* inductive reactive power through inverter 2. From t_2 to t_3, the PCC voltage is regulated at around 1.055 *pu* by absorbing 2 *pu* inductive reactive power capacity of inverter 2 as shown in Figure 6(b). From t_3 to 1.4 seconds, the PCC voltage is raised from 0.925 to 0.948 *pu* by injecting capacitive reactive power of 2 *pu* as shown in Figure 6(c). The droop coefficient for this method is 0.01 *pu*/*MVAR*. Figure 6(d) shows the total apparent power S handled by feeder 2. The Q-V droop method

utilizes the full inverter rating to compensate for voltage rise and voltage drop; a low X/R ratio system would require higher capacity of inverter to regulate the PCC voltage below the set margin of ±5%.

3.3. System Performance with P-Q-V Droop Control Method

Figure 7 shows the performance of feeder 2 with P-Q-V droop control method. The conditions for the PCC voltage before compensation are kept identical to those for P-f and Q-V droop method. From t_1 to t_2 the PCC voltage is reduced from 1.035 *pu* to 1.025 *pu* as shown in Figure 7(a) by absorbing 1.0 *pu* inductive reactive power through inverter 2. The active power coefficient is 0 since the controller mainly uses the reactive power for compensation; the reactive power coefficient is 0.04 *pu*/MVAR. From t_2 to t_3, the PCC voltage is regulated at 1.04 *pu* by absorbing 1.4 *pu* inductive reactive power and 0.8 *pu* active power as shown in Figure 7(b). The active droop coefficient is 0.08 *pu*/MW, while the reactive power coefficient is 0.018 *pu*/MVAR. The reactive power coefficient is thus reduced as more reactive power is absorbed from the inverter. From t_3 to 1.4 seconds, the PCC voltage is increased from 0.925 *pu* to 0.96 *pu* by injecting 1.4 *pu* capacitive reactive power and 0.7 *pu* active power simultaneously as shown in Figure 7(c). The active droop coefficient is 0.1 *pu*/MW, while the reactive power coefficient is 0.024 *pu*/MVAR. Figure 7(d) shows the total apparent power S handled by feeder 2. The inverter capacity is efficiently utilized for voltage regulation with the P-Q-V method than with P-f or Q-V droop methods individually.

4. Conclusion

In this article, different droop control methods for PV-based communal grid networks with different line resistances (R) and impedances (X) have been modelled and simulated in MATLAB to determine the most efficient control method for a given network. The results show that active power-frequency (P-f) droop control method is the most efficient for low voltage transmission networks with

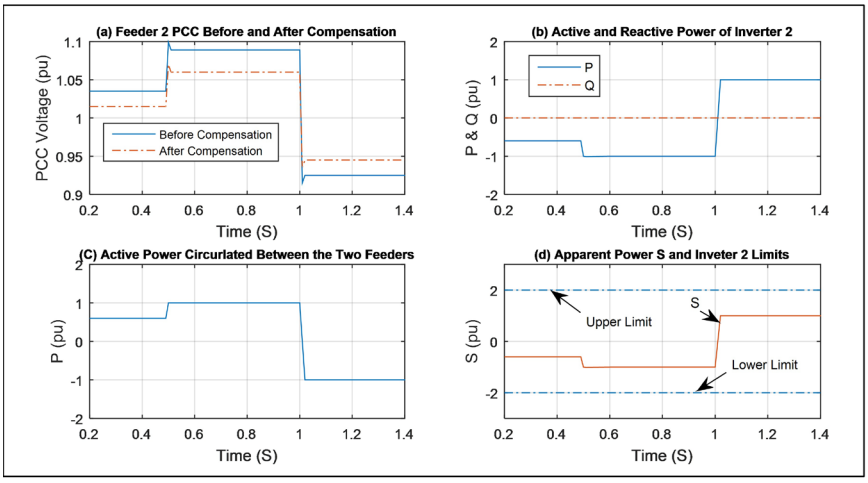

Figure 5. Feeder 2 performance using P-f droop control method.

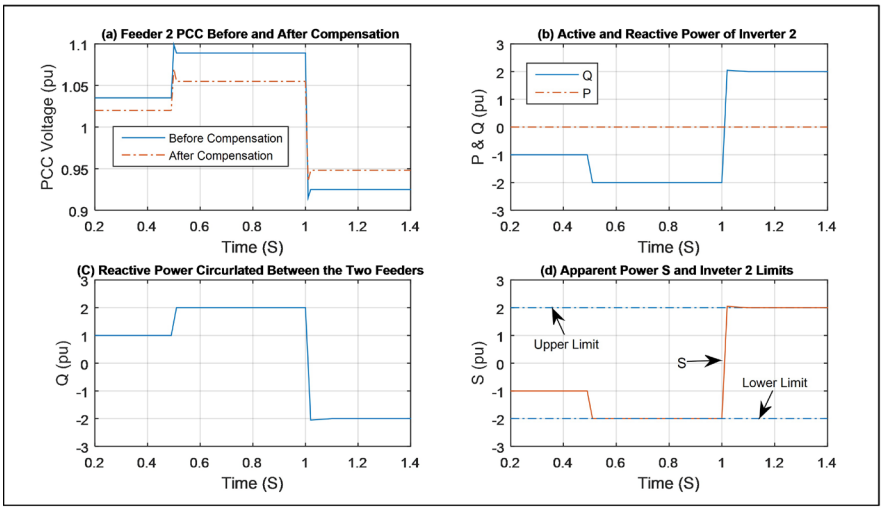

Figure 6. Feeder 2 performance using Q-V droop control method.

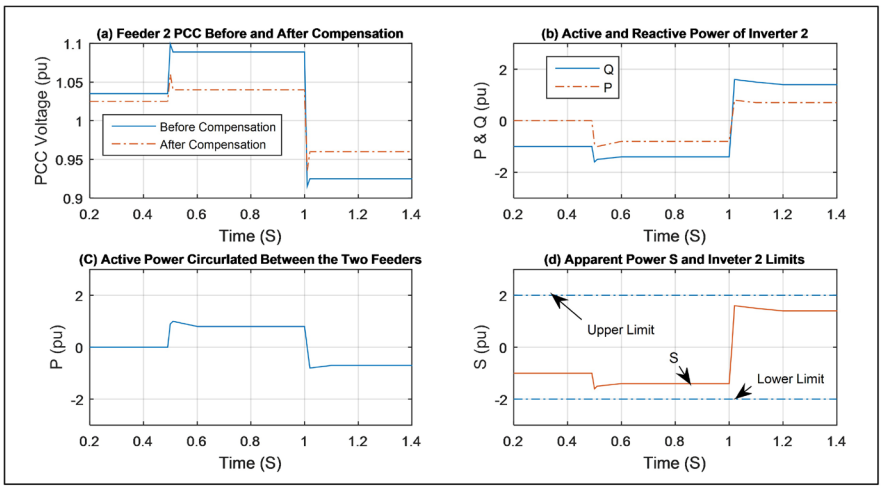

Figure 7. Feeder 2 performance using P-Q-V droop control method.

low X/R ratios while reactive power-voltage (Q-V) droop control method is the most efficient for systems with high X/R ratios. Results also show that P-f or Q-V droop control methods cannot individually efficiently regulate line voltage and frequency for systems with complex line resistances and impedances, *i.e.* near unity X/R ratios. For such systems, P-Q-f droop control method, where both active and reactive power could be used to control PCC voltage via shunt-connected inverters, is determined to be the most efficient control method. Results also show that shunt-connection of inverters leads to improved power flow control of interconnected communal grids by allowing feeder voltage regulation, load reactive power support, reactive power management between feeders, and improved overall system performance against dynamic disturbances. The necessary active power for the compensation is drawn from the interconnected feeders via the inverters. The controller then circulates minimum active power between the feeders while the active and reactive power droop coefficients are adjusted online through a look up table based on the PCC voltage level. A real-time integration

inductor-capacitor-inductor (LCL)-filter with a virtual inductance is used to actively damp the inverter output without the need for extra sensors to feedback measured signals.

Highlights

- *P-f* droop control method is suitable for networks with low *X*/*R* ratios.
- *Q-V* droop control method is suitable for networks with high *X*/*R* ratios.
- *P-Q-f* droop control method is suitable for networks with near unity *X*/*R* ratios.
- Shunt-connected inverters lead to improved system performance.

Acknowledgements

This research was funded by Leeds International Research Scholarship.

Conflicts of Interest

The authors declare no conflicts of interest regarding the publication of this paper.

References

[1] Huang, W., Lu, M. and Zhang, L. (2011) Survey on Microgrid Control Strategies. *Energy Procedia,* **12**, 206-212. https://doi.org/10.1016/j.egypro.2011.10.029

[2] Hatziargyriou, N. (2014) Microgrids: Architecture and Control. F. Edition, John Wiley & Sons, New York.

[3] Huang, J., Jiang, C. and Xu, R. (2008) A Review on Distributed Energy Resources and Microgrids. *Renewable and Sustainable Energy Review*, **12**, 2472-2483. https://doi.org/10.1016/j.rser.2007.06.004

[4] Basak, P., Saha, A. and Chowdhury, S. (2009) Microgrid: Control Techniques and Modelling. *Proceedings of the* 44*th International Universities Power Engineering Conference* (*UPEC*), Glasgow, 1-4 September 2009, 1-5.

[5] Pedrasa, M. and Spooner, T. (2006) A Survey of Techniques Used to Control Microgrid Generation and Storage during Island Operation. 16th *Australasian Universities Power Engineering Conference* (*AUPEC*2006), Melbourne, 10-13 December 2006.

[6] De Brabandere, K. and Bolsens, B. (2007) A Voltage and Frequency Droop Control Method for Parallel Inverters. *IEEE Transaction on Power Electronics*, **22**, 1107-1115. https://doi.org/10.1109/TPEL.2007.900456

[7] (2003) Renewable Academy (RENAC), ReGrid: Frequency and Voltage Regulation in Electrical Grids. http://docplayer.net/6038884-Regrid-frequency-and-voltage-regulation-in-electrical-grids.html

[8] Bevrani, H. and Shokoohi, S. (2013) An Intelligent Droop Control for Simultaneous Voltage and Frequency Regulation in Islanded Microgrids. *IEE Transactions on Smart Grid*, **4**, 1505-1514. https://doi.org/10.1109/TSG.2013.2258947

[9] Pecas-Lopes, J., Moreira, C. and Mandureira, A. (2006) Defining Control Strategies for Microgrids Islanded Operation. IEEE Transactions on Power Systems, **21**, 916-924. https://doi.org/10.1109/TPWRS.2006.873018

[10] Pecas-Lopes, J., Moreira, C., Mandureira, A., *et al.* (2005) Control Strategies for Microgrids Emergency Operation. *International Conference on Future Power Systems*, Amsterdam, 18 November 2005, 6 p. https://doi.org/10.1109/FPS.2005.204226

[11] Ashbani, S. and Abdel-Rady, M. (2013) General Interface for Power Management of Micro-Grids Using Nonlinear Cooperative Droop Control. *IEEE Transactions on Power Systems*, **20**, 2929-2941. https://doi.org/10.1109/TPWRS.2013.2254729

[12] Bergen, A. and Vittal, V. (1999) Power Systems Analysis. Prentice Hall, NJ, USA.

[13] Engler, A. and Soultanis, N. (2005) Droop Control in LV-Grids. *International Conference on Future Power Systems*, Amsterdam, 18 November 2005, 6 p. https://doi.org/10.1109/FPS.2005.204224

[14] Yao, W. and Chen, M. (2011) Design and Analysis of the Droop Control Method for Parallel Inverters Considering the Impact of the Complex Impedance on the Power Sharing. *IEEE Transactions on Industrial Electronics*, **58**, 576-588. https://doi.org/10.1109/TIE.2010.2046001

[15] Alatrash, H., Mensah, A., Mark, E., *et al.* (2011) Generator Emulation Controls for Photovoltaic Inverters. 8*th International Conference on Power Electronics*—ECCE, Asia, 30 May-3 June 2011, 996-1011. https://doi.org/10.1109/ICPE.2011.5944502

[16] Abusara, M., Shark, S. and Guerrero, J. (2015) Improved Droop Control Strategy for Grid-Connected Inverters, Sustainable Energy. *Grida and Networks*, **1**, 10-19.

[17] Vallve, X. and Serrasolses, J. (1997) Design and Operation of a 50 kWp PV Rural Electrification Project for Remote Sites in Spain. *Solar Energy*, **59**, 111-119. https://doi.org/10.1016/S0038-092X(96)00124-7

[18] Chaurey, A. and Kandpal, T. (2010) A Techno-Economic Comparison of Rural Electrification Based on Solar Home Systems and PV Microgrids. *Energy Policy*, **38**, 3118-3129. https://doi.org/10.1016/j.enpol.2010.01.052